Membrane curvature studied using two-dimensional NMR in fluid lipid bilayers

François Macquaire and Myer Bloom
Department of Physics, University of British Columbia, 6224 Agricultural Road, Vancouver, British Columbia, Canada V6T 1Z1
(Received 12 October 1994)

The method of two-dimensional exchange spectroscopy in deuterium (^{2}H) nuclear magnetic resonance (NMR), originally developed for the study of slow, reorientational molecular motions in solids [S. Wefing and H. W. Spiess, J. Chem. Phys. **89**, 1219 (1988)], has been applied to the study of multilamellar vesicle samples of phospholipid bilayer systems in their fluid (L_α) phase. As is well known, the ^{2}H NMR quadrupolar splitting in such fluid membranes is proportional to $(3\cos^2\theta - 1)$, where θ is the angle between the local bilayer surface normal and the external magnetic field. Measurements of two-dimensional exchange ^{2}H NMR spectra using a mixing time t_m were analyzed to give the reorientational angle distribution function for the local surface normals of individual lipid molecules comprising the membranes. A quantitative analysis of this correlation function taking into account the lateral diffusion of the lipid molecules demonstrated the sensitivity of the technique to the local curvature and shapes of the multilayers, which were shown to exhibit surface roughness on the mesoscopic length scale between about 10 nm and 1 μm. The results were consistent with an average radius of curvature between 1 and 2 μm, but approximately 15% of the molecules were located on relatively flat membranes having larger radii of curvature.

PACS number(s): 61.30.−v, 76.60.−k, 87.22.−q

I. INTRODUCTION

An important physical feature of the lipid bilayer core of biological membranes is that it is almost always fluid under physiological conditions. This fluid characteristic is responsible for the extreme softness of many biological materials, which leads to a complex interplay between structure and dynamics at length scales ranging from the molecular (≤ 1 nm) to the size of biological cells (≥ 1 μm). Associated with this range of distances is an even more impressive range of correlation times τ_c for membrane dynamical processes extending over at least 12 orders of magnitude from picoseconds for some internal molecular motions to several seconds for shape and curvature fluctuations extending over cell-size distances [1,2].

Different spectroscopic and other physical measurements are sensitive to different time and distance scales. In some cases, the origin of the intrinsic time and distance scale of a technique is subtle [3]. For example, in the case of fluid membranes, an interesting NMR length scale L_{NMR} in the range of about 100 to 1000 Å obtains as a consequence of the lateral diffusion of the lipid molecules parallel to the plane of the membrane. A natural NMR "time scale" τ_{NMR} is set by the magnitude of the spin-dependent interactions responsible for broadening and splitting of the spectral lines. τ_{NMR} turns out to be of the same order of magnitude for ^{1}H, ^{2}H, and ^{31}P NMR in membranes ($\approx 10^{-5}$ s). Fast motions, i.e., those with $\tau_c \ll \tau_{\mathrm{NMR}}$, result in spectral characteristics representing averages over the motions. In order to record meaningful spectra, the NMR free induction signal must be sampled for a time somewhat longer than τ_{NMR}, during which the molecules diffuse a distance $L_{\mathrm{NMR}} \geq (4D\tau_{\mathrm{NMR}})^{1/2}$. The values of L_{NMR} given above correspond to values of the lateral diffusion constant in the vicinity of $D \approx 4\times 10^{-12}$ $\mathrm{m^2\,s^{-1}}$, which is typical of phospholipid molecules in fluid membranes.

In this paper, we are concerned with membrane shape and curvature considerations for which the most direct information has been provided by optical measurements (see, e.g., Refs. 1–9 in [4]). Optical measurements are especially powerful for shape fluctuations occurring over cell-size distances (≈ 1–10 μm). In this range, the relevant correlation time τ_c is of order seconds for unilamellar vesicles, scaling as λ^3 for fluctuations characterized by a wavelength λ [5]. Equilibrium mechanical measurements indicate that surface undulations and their related shape and curvature fluctuations occur over a wide range of λ extending all the way down from the cell size to the bilayer thickness of about 50 Å [1]. Up to now, very few direct measurements have been carried out in the suboptical, mesoscopic range, $\lambda \leq 4000$ Å. Some indirect information is available, including that obtained from ^{3}H NMR measurements of the transverse relaxation time T_2 [1,6].

The information arising from the use of two-dimensional exchange ^{2}H NMR measurements, described here and in the accompanying paper on solid-supported spherical bilayers of fluid membranes [7], is on a different footing from previous studies of the mesoscopic range of distances since it provides a direct quantitative measure of the space-time correlation function of the orientation of local surface normals for individual molecules.

II. THE TWO-DIMENSIONAL EXCHANGE ^{2}H NMR EXPERIMENT IN MEMBRANES

In two-dimensional (2D) NMR experiments, the phases of spins are first labeled in terms of their initial spectral frequency ω_1 via a *preparation sequence,* the molecular positions and internal coordinates are then allowed to evolve for a time t_m during a *mixing period,* and, finally,

 ©1995 The American Physical Society

the *free induction decay* (FID) signal giving the spectral frequency ω_2 after the mixing period is recorded during the subsequent *detection period.* The 2D NMR spectrum $S(\omega_1,\omega_2;t_m)$ so defined gives the joint probability that a given spin has spectral frequencies ω_1 and ω_2 at times separated by t_m.

In the case of fluid membranes, there exists a direct connection between this 2D ^{2}H NMR spectrum and membrane geometry because of the well established relationship between ω_i and the angle θ_i between the surface normal **n** and the external magnetic field, namely,

$$\omega_i=\Omega_q P_2(\cos\theta_i)=\omega_q S_{\mathrm{CD}} P_2(\cos\theta_i)$$
$$=\omega_q S_{\mathrm{CD}}(3\cos^2\theta_i-1)/2\ , \qquad (1)$$

where ω_q is the quadrupolar coupling frequency and S_{CD} is the orientational order parameter for the C—D bond. As shown by Spiess and co-workers [8–11] and reviewed in our Materials and Methods section, measurements of $S(\omega_1,\omega_2;t_m)$ can be analyzed to yield the joint probability $P(\theta_1,\theta_2;t_m)$ that **n** is oriented at θ_1 initially and at θ_2 at a time t_m later. Moreover, in the case of an axially symmetric coupling tensor in a powder sample, the information contained in the experimental data can be expressed by a one-dimensional distribution function $P(\beta;t_m)$, where β stands for the change of angle of the symmetry axis (**n** in our case) during t_m. Such changes can occur as a result of dynamical membrane processes leading to changes in local curvature and/or molecular diffusion that transports individual molecules from one part of a curved membrane to another. This latter diffusion process can lead to the determination of local membrane geometry over distances $L \geq L_{\mathrm{NMR}}$, a relatively unexplored region of distances, as noted in the Introduction.

The method of Spiess involves sequences of three pulses, or slightly modified sequences of the type used here, i.e.,

$$90_y\text{-}t_1\text{-}54_\phi\text{-}t_m\text{-}54_\phi\text{-}\delta\text{-}90_x\text{-}\delta\text{-}t_2$$

(2D exchange ^{2}H NMR pulse sequence), where t_1 and t_2 define evolution and detection periods and the 90_x pulse is a pulse superimposed on the Spiess three-pulse sequence to refocus the FID signal for reasons described in the next section. In the above pulse sequence, the notation θ_ϕ characterizes a pulse that rotates the nuclear magnetization by an angle θ about an axis in the x-y plane making an angle ϕ with the x axis. Thus, 90_x corresponds to a 90° rotation about the x axis.

The pulse sequence is applied to the ^{2}H spin system, initially in equilibrium with a heat reservoir in the presence of a large magnetic field along the z axis. Because the ^{2}H quadrupolar interaction is normally at least two orders of magnitude smaller than the Zeeman interaction, these initial conditions imply that, initially, the spin system has a nonzero vector polarization $\langle I_z\rangle_0=I_0$ and a negligibly small tensor (quadrupolar) polarization, i.e., $\langle 3I_z^2-I(I+1)\rangle_0\approx 0$. Then, the first two pulses store vector or tensor spin polarization in an "invariant of the motion" proportional to $\cos[\omega_1 t_1]$ *or* $\sin[\omega_1 t_2]$ depending on whether the phase of the second pulse is $\phi=y$ or x, respectively. After the mixing period, application of a third pulse identical to the second results in a contribution of the spin to the FID signal of the form

$$F_{cc}(t_1,t_2)=A_c\cos[\omega_1 t_1]\cos[\omega_2 t_2]$$

or (2)

$$F_{ss}(t_1,t_2)=A_s\sin[\omega_1 t_1]\sin[\omega_2 t_2]$$

for the two phase settings given above, respectively. In the absence of relaxation effects that are dependent on ω_i; the amplitudes A_c and A_s are equal for the choice of 54° for the rotation angle of the second and third pulses in the pulse sequence shown above. For a system of many spins, the FID signals actually measured represent sums over ω_1 and ω_2 for all the spins in the sample.

By recording the two types of FID's, i.e., $F_{ll}(t_1,t_2)$, $l\in\{c,s\}$, over a wide enough range of values of t_2, repeating the measurements for each value of t_1 in a corresponding range of t_1 values, and calculating the two-dimensional Fourier transform over t_1 and t_2, one obtains the pure absorption 2D ^{2}H NMR spectrum $S(\omega_1,\omega_2;t_m)$ ultimately required to obtain the maximum amount of dynamical information on membrane geometry from $P(\beta;t_m)$. The numerical procedures required to obtain $P(\beta;t_m)$ from $S(\omega_1,\omega_2;t_m)$ are reviewed in the next section.

III. MATERIALS AND METHODS

A. Composition and preparation of the samples

The 1-palmitoyl-d_{31}-2-oleoyl-*sn*-glycero-3-phosphatidylcholine (POPC-d_{31}), in which the palmitoyl chain is fully deuterated, was purchased from Avanti Polar Lipids Inc. (Birmingham, AL), while 1,2-dipalmitoyl-*sn*-glycero-3-phosphatidylcholine (DPPC-d_2), headgroup deuterated in the α position, was kindly provided by Dr. M. Roux.

Multilamellar NMR samples were prepared in the usual manner as follows. The appropriate dry weight of lipids was dissolved in deuterium-depleted water and then extensively vortexed. In addition, the DPPC-d_2 samples were submitted to three freezing (liquid nitrogen) and thawing (50 °C) cycles, centrifuged, and the pellet transferred directly into the NMR tube.

B. NMR experimental methods

The ^{2}H NMR spectra were recorded on a home-built 46 MHz spectrometer described in detail elsewhere [12,13]. Two-dimensional exchange experiments were carried out using the method outlined by Schmidt, Blümlich, and Spiess [14]. However, the pulse phase cycle was modified to match the receiver phase in the 8-CYCLOPS sequence [15]. This sequence of transmitter and receiver phases is commonly used [17] to eliminate various artifacts associated with quadrature detection in ^{2}H NMR. The separation between the two-pulse preparation sequence and the third pulse (i.e., the mixing time t_m in the pulse sequence shown in the preceding section) was varied from 100 μs to 10 ms and a refocusing pulse (not shown) was applied 30 μs after the third pulse

to circumvent the receiver dead time, in analogy to what is done in a quadrupolar echo experiment [16]. Normally, 4096 transients were acquired with a recycling delay of 200 ms. A total of 128 increments of 256 data points was collected for each 2D experiment, yielding a digital resolution of 976 Hz for each of the equally spaced intervals in each of the two dimensions after zero filling, corresponding to a dwell time of 4 μs and a sweep width of about 200 kHz. In order to start both Fourier transformations from $t_1=t_2=0$ and avoid phase distortions, the experimental data were successively time shifted prior to the Fourier transformation [17].

C. Reconstruction of the angular distribution function from ^{2}H NMR experiments

In the slow motion limit, the time-dependent, experimental, two-dimensional FID signal of Eq. (1) for an axially symmetric quadrupolar coupling tensor can be written in terms of the evolution and detection times t_1 and t_2, respectively, as [8–11]

$$F_{ll}(t_1,t_2)=\int_0^{\pi/2}K_{ll}(t_1,t_2|\beta)e^{-(t_1+t_2+2\delta)/T_2}\times[P(\beta)+P(\pi-\beta)]d\beta\ . \tag{3}$$

Equation (3) requires considerable explanation. A single exponential decay of the transverse magnetization has been assumed and characterized by the time constant T_2. The Kernel functions $K_{ll}(t_1,t_2|\beta)$, $\{l\}\in\{c,s\}$, are defined by [8–11] as follows:

$$K_{cc}(t_1,t_2|\beta)=\frac{1}{\pi}\int_0^1 db\int_0^\pi d\alpha\cos[\Omega_q g(b)t_1]\times\cos[\Omega_q h(\alpha,b,\beta)t_2] \tag{4}$$

and

$$K_{ss}(t_1,t_2|\beta)=\frac{1}{\pi}\int_0^1 db\int_0^\pi d\alpha\sin[\Omega_q g(b)t_1]\times\sin[\Omega_q h(\alpha,b,\beta)t_2]\ , \tag{5}$$

where Ω_q has been defined in Eq. (1). The quantities g and h are expressed, in a manner that follows from the addition theorem for spherical harmonics, in terms of $b=\cos\theta_1$ and the polar and azimuthal angles β and α associated with the change in the orientation of $\mathbf{n}$ from its initial value $\mathbf{n}_1$ to its value $\mathbf{n}_2$ as a result of its motion relative to $\mathbf{n}_1$ during the mixing period,

$$g(b)=\tfrac{1}{2}(3b^2-1)\ , \tag{6}$$

$$h(\alpha,b,\beta)=\tfrac{3}{4}(1-b^2)\sin^2\beta\cos2\alpha-3b(1-b^2)^{1/2}\sin\beta\cos\beta\cos\alpha+\tfrac{1}{4}(3b^2-1)[3\cos^2\beta-1]\ . \tag{7}$$

The reorientational angle distribution (RAD) function $P(\beta;t_m)$ gives the probability that the motionally averaged axis of symmetry $\mathbf{n}$ for a given molecule jumps by an angle β during the mixing time. Quantitative information on $P(\beta;t_m)$ is the most important outcome of 2D exchange ^{2}H NMR experiments on membranes. Due to the symmetry properties of the orientation dependence of the quadrupolar splitting, jumps of angle β change the 2D spectrum in a manner that is indistinguishable from jumps of $\pi-\beta$. Therefore the 2D exchange experiments can only be used to determine the symmetrized RAD function $P^*(\beta)$ defined by

$$P^*(\beta)=P(\beta)+P(\pi-\beta)\ . \tag{8}$$

The back calculation procedures giving the function $P^*(\beta)$ from the 2D spectrum were performed in the frequency domain. First, the time domain Kernel functions were computed via numerical integration of Eqs. (4) and (5). In the analysis of the experimental data, 128 increments of 256 data points were computed for each function, yielding a digital resolution equal to the experimental spectrum after zero filling. Then the subspectra $s(\omega_1,\omega_2|\beta)$ were obtained by processing the corresponding Kernel functions with the same procedures used for the experimental spectrum $S(\omega_1,\omega_2)$. Finally, the modified RAD function was obtained by optimizing, under constraints, the squared Euclidean distance [18]

$$R=\sum_{\omega_1\omega_2}[S(\omega_1,\omega_2)-\sum_\beta P^*(\beta)s(\omega_1,\omega_2|\beta)]^2\ , \qquad P^*(\beta)\geq0\ . \tag{9}$$

In all cases, 30 subspectra were computed leading to an accuracy of 3° for the β angles. The stability of the algorithm was thoroughly tested for simulated spectra and for the well known 2D pattern displayed by the fully deuterated dimethylsulfon sample [14].

IV. RESULTS AND DISCUSSION FOR SPECIFICALLY LABELED LIPIDS

A. Slow motions in multilamellar vesicles detected by 2D exchange ^{2}H NMR experiments

As described in the last section, it is necessary to determine experimentally the two functions $F_{cc}(t_1,t_2)$ and $F_{ss}(t_1,t_2)$ in order to obtain maximal information via 2D NMR on dynamic properties of systems such as membranes. This is especially true of powder samples such as those studied here, in which all initial orientations θ_1 of $\mathbf{n}$ are equally probable. The two data sets are combined, after being processed, to give a pure absorption spectrum. We assumed in the numerical analysis procedure described in Sec. III that frequency exchange may be neglected during the preparation and detection periods, so that the 2D exchange spectrum depends only on the mixing time and may be written in the form of a two-time distribution function $S(\omega_1,\omega_2;t_m)$, which is interpreted as the joint probability of individual nuclei having frequencies ω_1 and ω_2 at times separated by t_m. Arguments justifying this approximation for the system studied here are presented below. For a demonstration of the systematic errors introduced by this approximation for diffusive motions on a sphere, see the accompanying paper [7].

In the case of discrete jump motions, characteristic ridges such as ellipsoids are observed for such experiments on powders [19,20]. However, for more complex motions of the type likely to be of importance in membranes, e.g., diffusive processes or random fluctuations of

the local director orientation, more complex patterns are anticipated—and observed. Computer simulations have been used to describe quantitatively the 2D spectra to be expected for molecules diffusing on spherical surfaces [7–9,21]. We shall compare such simulations with our measurements of phospholipid molecules in fluid lipid bilayer membranes in which one can say with confidence that diffusional motions along the curved surfaces must be one of the important motions taking place.

Figure 1 shows a set of spectra $S(\omega_1,\omega_2;t_m)$ from 2D exchange ^{2}H NMR experiments recorded at 50 °C on DPPC-d_2 molecules deuterated in the α position of the headgroup. The stacked plots and the corresponding contour plots presented in Fig. 1 exhibit the evolution of the 2D spectra as the mixing time is incremented over the values $t_m=100$ μs, 1.0, 5.0, and 10.0 ms. Some general features of these spectra deserve comment before discussing the detailed numerical analysis of the data.

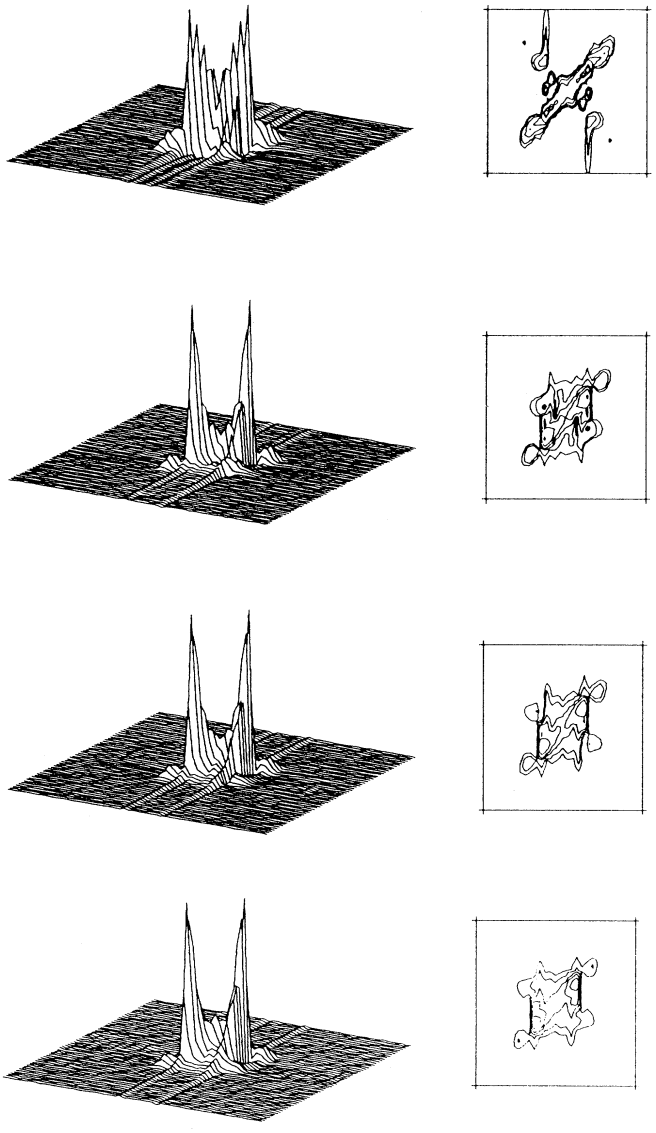

FIG. 1. 2D exchange ^{2}H NMR spectra of multilamellar DPPC-d_2 at 50 °C in the fluid (L_α) phase. The stacked plots (left) and corresponding contour plots (right) refer, from top to bottom, to mixing times of $t_m=100$ μm, 1.0, 5.0, and 10.0 ms, respectively. The plots of the stacked plots along each of the two dimensions range from −28 to +28 kHz while those of the contour plots range from −15 to +15 kHz in each dimension. The abscissae correspond to the frequencies $f_1=\omega_1/2\pi$ and the ordinates to $f_2=\omega_2/2\pi$.

(i) Each of the four spectra exhibits reflection symmetry with respect to the antidiagonal. This reflects the presence of two NMR transitions, symmetric with respect to the Larmor frequency, for the ^{2}H ($I=1$) nucleus due to the quadrupolar interaction.

(ii) Whereas the 2D spectral intensity is mainly located on the main diagonal for the shortest mixing time of $t_m=100$ μs, the off-diagonal intensities become more important as t_m is increased and are dominant at the largest value of $t_m=10$ ms used in our experiments. Furthermore, the large off-diagonal components at $(\omega_1,\omega_2)=(\Omega_q,-\frac{1}{2}\Omega_q)$ observed in the $t_m=10$ ms spectrum reveals that a significant fraction of the symmetry axes of the lipid molecules rotate by more than 90° during the 10 ms mixing time. A formal way of expressing this in terms of the numerical analysis of Sec. III is that there must be substantial values of $P^*(\beta;t_m)$ for $\beta=90°$ and $t_m=10$ ms.

At 50 °C, the lipid molecules in our DPPC sample are in the liquid crystalline (L_α) phase and organized in multilamellar vesicles, having a wide range of sizes with average size in the vicinity of 1–2 μm. Typical values of the lateral diffusion constant in L_α phase membranes have been found to be in the range $10^{-11}\geq D\geq 10^{-12}$ m^2/s [22]. For the DPPC-d_2 sample studied here, $D\approx 4\times 10^{-12}$ m^2 s^{-1} [23]. A measure of the correlation time for diffusion of molecules around a sphere of radius R is $\tau_2=R^2/6D$, which for the diffusion constant given above and for $0.5\leq R\leq 1.0$ μm gives $10\leq\tau_2\leq 40$ ms. Thus the observation of substantial values of $P^*(90°;10$ ms) is consistent with diffusive motions around curved surfaces of radii $R\leq 1$ μm making appreciable contributions to $P^*(\beta;t_m)$.

In view of the known complexity of shapes in multilamellar vesicle dispersions, we do not anticipate being able to fit all of our observations to diffusion on a spherical surface. One may ask, however, whether the results can be fitted to a distribution of spherical particles. More interesting is whether our measurements are sensitive to surface roughness that is believed to be present on the mesoscopic length scale but for which there exists only indirect experimental evidence at the present time [1,6,7]. Fortunately, the method of analysis of our data by back calculation from the 2D spectrum [11,18] described in Sec. III allows us to extract $P^*(\beta;t_m)$ without assuming any specific motion or mechanism, and this is what we now proceed to do.

B. Determination of the $P^*(\beta;t_m)$ of DPPC-d_2 in the L_α phase from the 2D spectra

Figure 2 shows the modified RAD's, $P^*(\beta;t_m)$, extracted from the corresponding 2D spectra of DPPC-d_2 in Fig. 1 using the methods described in Sec. III and values of the quadrupolar splitting ($\Omega_q=2\pi\times 6.5$ kHz) and relaxation time ($T_2=1.2$ ms) parameters measured

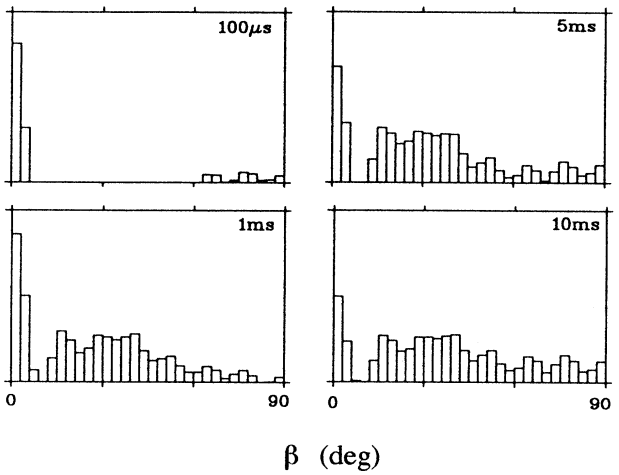

FIG. 2. Histograms of the reorientational distribution functions $P^*(\beta;t_m)$ expressed as functions of the reorientational angle β in degrees between $\beta=0°$ and $\beta=90°$. As discussed in the text, $P^*(\beta;t_m)=P^*(\pi-\beta;t_m)$. These functions were extracted by numerical analysis of the experimental spectra in Fig. 1, as described in the text. The $t_m=1.0$, 5.0, and 10.0 ms plots are normalized and have the same scaling factor, which differs from that for $t_m=100$ μs.

elsewhere [23].

In reality, T_2 in this system is strongly orientation dependent as measured by the normal (1D) spin echo method and the value of $T_2=1.2$ ms is based on the orientation-averaged relaxation rate

$$\langle 1/T_2\rangle = A + B\langle \sin^2\theta\cos^2\theta\rangle ,$$

with $A=300\ s^{-1}$ and $B=6700\ s^{-1}$ [23,24]. We justify neglect of the orientation dependence of T_2 in this case with the *ad hoc* argument that the powder line shapes from quadrupolar echoes are not strongly affected by such orientational dependence under the conditions (values of t_1, t_2, and δ) of our experiments. Further work remains to be done on the importance of such orientation dependence of T_2 obtained from 1D measurements on the interpretation of 2D exchange spectra, but it is likely that it plays a much smaller role in cases such as this than one might initially guess. The reason for this is that part of the orientation dependence of T_2 in this system is associated with the random frequency modulation associated with the slow transfer of magnetization between different parts of the ^{2}H NMR spectrum, i.e., the very processes of magnetization exchange that we have measured in a 2D NMR experiment manifest themselves as a T_2 mechanism in a 1D experiment. From this argument, it would appear that exchange processes that result in a decrease in total NMR (echo) intensity in a 1D experiment do not necessarily lead to a loss of total intensity in a 2D experiment.

The $P^*(\beta;t_m)$ are related via Eq. (8) to the RAD probabilities $P(\beta;t_m)d\beta$ that the local surface normal of a molecule changes its orientation by an angle between β and $\beta+d\beta$ during the mixing time. For diffusive and other quasicontinuous processes, $P^*(\beta;t_m)$ is expected to converge towards $P(\beta;t_m)$ in the short time limit, and also for large values of t_m when complete randomization of the molecular orientations is attained.

Meaningful $P^*(\beta;t_m)$ values for $t_m=100$ μs were obtained despite the mixing time being so short that transients from the preparation pulse sequence were still quite large during the detection period. The absence of large off-diagonal intensities and the observation that almost all of the intensity of $P^*(\beta;100\ \mu s)$ is close to $\beta=0°$ validates the assumption, necessary to the back calculation, that no significant exchange occurred during the 100 μs mixing time and, hence, that the quadrupolar splittings do not change significantly during the preparation and detection periods. The low intensity contributions observed for large values of β in $P^*(\beta;100\ \mu s)$ are almost certainly artifacts arising from such transients and their magnitude should be completely negligible for the larger values of $t_m=1.0$, 5.0, and 10.0 ms used in the other experiments.

As shown in Fig. 2, $P^*(\beta;1.0\text{ ms})$ exhibits a maximum located near 30° that reflects a fast component of the reorientational process. By contrast, the substantial value of $P^*(\beta;1.0$ ms) in the first two β channels, i.e., $0°\le\beta\le 6°$, indicates that the local surface normals for about 30% of the molecules do not change their orientation by a measurable amount during 1 ms. As is evident from an examination of $P^*(\beta;5.0$ ms) and $P^*(\beta;10.0$ ms), the fraction of molecules *whose surface normal orientations do not change* gradually decreases as t_m is increased to 10 ms. Finally, the continuous displacement of $P^*(\beta;t_m)$ towards the $\beta=90°$ reorientation reflects the large change of local surface normal orientation experienced by a large number of the molecules.

C. Model of molecules diffusing on spherical surfaces

It is clear that the processes leading to the experimentally measured values of $P^*(\beta;t_m)$ are too complex to be represented by molecules diffusing on a single spherical surface. In such a case, solution of the diffusion equation for molecules diffusing with diffusion constant D on a sphere of radius R gives

$$P(\beta;t_m)=\tfrac{1}{2}\sum_{l=0}^{\infty}(2l+1)P_l(\cos\beta)\exp[-t_m/\tau_l]\sin\beta \tag{10}$$

with

$$1/\tau_l = l(l+1)D/R^2 . \tag{11}$$

This form of $P(\beta;t_m)$ was found, in the accompanying paper [7], to be in excellent agreement with measurements made on lipid bilayers supported on spherical glass beads using values of D and R from independent measurements.

We now ask whether the $P^*(\beta;t_m)$ of Fig. 2 can be interpreted sensibly in terms of a model of different populations of molecules diffusing on spherical surfaces of different radii, e.g., a fraction f_i of the molecules diffusing on a sphere of radius R_i, having a value of the diffusional correlation time $\tau_d(i)=\tau_2(i)=R_i^2/6D$.

The best two-component fit for $P^*(\beta;1.0$ ms) is shown

in Fig. 3. The fitting parameters are $f_1=0.75$ for the fast reorientation component having a correlation time of $\tau_d(1)=1.3$ ms and $f_2=0.25$ for the second component with a very long correlation time and accounting for the intensities of the first two channels of β.

Reasonable fits for $P^*(\beta;5.0\text{ ms})$ and $P^*(\beta;10.0\text{ ms})$, also shown in Fig. 3, require at least three components. If the shortest correlation time is fixed at $\tau_d(1)=1.3$ ms in each case to conform to the value obtained for $t_m=1.0$ ms, then the longer correlation time is found to be $\tau_d(2)=9.0$ and 14.0 ms, respectively, for the two cases with amplitude factors $f_1=0.25$ and 0.30, $f_2=0.6$ and 0.55 in each case, and $f_3=0.15$ for the unchanged, too-long-to-be-measured correlation time component.

We interpret the variation of both the amplitudes and correlation times in these fits as indicating that the model of a superposition of molecules diffusing on spheres of different radii does not fit. The dynamics of changes of local surface normals must involve more complicated shape considerations, a conclusion that should not surprise anyone familiar with electron micrographs of multilamellar vesicle dispersions.

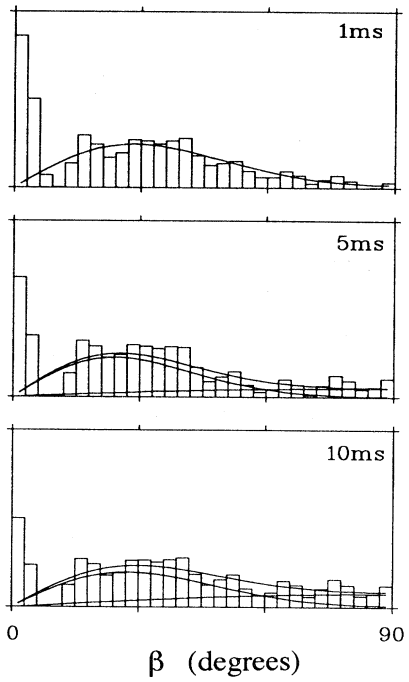

FIG. 3. Superposition of experimental RAD functions (histograms) calculated from 2D exchange ^{2}H NMR experiments and simulations (solid lines) from the isotropic rotational diffusion model. As in Fig. 2, the reorientational angle β is expressed in degrees. Three solid lines are displayed on each of the $t_m=5$ and 10 ms graphs representing the two correlation functions, characterized by $\tau_d(i)$, $i=1$ and 2, appearing in the best fit, as well as their sum. As described in the text, the correlation times and their associated lipid fractions are $\tau_d(1)=1.3$ ms and $f_1=0.75$ for the $t_m=1.0$ ms graph; $\tau_d(1)=1.3$ ms, $f_1=0.25$ and $\tau_d(2)=9$ ms, $f_2=0.60$ for the $t_m=5.0$ ms graph; $\tau_d(1)=1.3$ ms, $f_1=0.30$ and $\tau_d(2)=14$ ms, $f_2=0.55$ for the $t_m=10.0$ ms graph.

D. Interpretation in terms of rough surfaces and flattened liposomes

One plausible interpretation of our experimental data is that the measurements exhibit the combined effects of (i) radii of curvature in the range of 1–2 μm, consistent with electron micrograph studies of similar samples [26] (the $i=2$ components), (ii) radii of curvature $\gg 1$ μm due to about 15% of the membrane surfaces that are associated with flattened liposomes (the very long correlation time components), and (iii) relatively small angle tilting of the surface normals due to roughness of the membrane surfaces on a length scale $\ll 1$ μm (the $i=1$ components).

Further experimental study is required to test this interpretation and to motivate further mathematical modeling of the distribution of membrane shapes. We confine ourselves here to some comments on the length scale of the surface roughness proposed in (iii). Suppose that $P(\beta_r;t_m)$, the distribution of tilt angles β_r associated with surface roughness, is sampled by a diffusive process governed by a correlation time τ_{cr}; either the molecules diffuse over the bumpy membrane or the bumps diffuse past the molecules. We represent $P(\beta_r;t_m)$ empirically as a Gaussian distribution with the limiting behavior for its variance at short and long times of the form expected for a diffusive process involving a bounded random variable, i.e., $\langle\beta_r^2\rangle \le \beta_M^2 \ll 1$,

$$\langle\beta_r^2\rangle=\beta_M^2[1-\exp(-t_m/\tau_{cr})] \tag{12}$$

$$\approx \begin{cases}[\beta_M^2/\tau_{cr}]t_m & \text{for } t_m \ll \tau_{cr} \quad (12a)\\ \beta_M^2, \text{ independent of } t_m & \text{for } t_m \gg \tau_{cr}\,. \quad (12b)\end{cases}$$

Interpreting the $i=1$ component of $P^*(\beta;1.0\text{ ms})$ in Fig. 3 in terms of Eqs. (12) for $t_m \ge \tau_{cr}$, one obtains $\beta_M \ge 0.5$ rad and $\tau_{cr} \le 1$ ms. For a diffusive process, the correlation time is related to the correlation length λ of the surface roughness and the diffusion constant D, approximately, via $\tau_{cr} \approx \lambda^2/2D$. If D is identified with the diffusion constant of the fluid membrane, $D \approx 4\times10^{-12}$ $\text{m}^2\,\text{s}^{-1}$, the inequality $\tau_{cr} \le 1$ ms gives an upper limit $\lambda \le 900$ Å (90 nm).

The shape and topology of the membrane surface are probably more complex than implied by this simple interpretation. We emphasize one feature that is definitely required to fit our experimental results. The fact that the fast motion of the $i=1$ component of $P^*(\beta;1.0\text{ ms})$ splits into at least two components implies that molecules are transferred by dynamical membrane processes, presumably diffusion, from more to less highly curved regions. Also, the fact that about 15% of the molecules remain at membrane positions with unchanged surface normal orientations implies the existence of some relatively flat membrane regions.

V. EXPERIMENTAL STUDIES USING PERDEUTERATED ACYL CHAINS

As shown in the previous section, correlation functions of slow motions in fluid lipid bilayer systems between

states having different orientations of local surface normals, can be determined quantitatively and unambiguously from 2D exchange ^{2}H NMR experiments on selectively deuterated molecules. In principle, such information should also be obtainable from more complex spin systems such as perdeuterated acyl chains and dipolar coupled proton spin systems. Because of the more complex NMR spectrum, it is not obvious that an unambiguous determination of $P^*(\beta;t_m)$ can be carried out in these cases even though the spin Hamiltonian leading to the NMR spectrum scales as $P_2(\cos\theta)$ in fluid bilayer membranes [25]. If it does eventually turn out to be possible to determine $P^*(\beta;t_m)$ from ^{1}H NMR, the study of an important class of slow motions in biological membranes would be opened up for investigation. In this short section, we report some preliminary results on this problem using POPC-d_{31} membranes.

Figure 4 presents the 2D exchange ^{2}H NMR spectra for POPC-d_{31} at 30 °C for mixing times $t_m=1.0$ and 10.0 ms. The spectra of Fig. 4 are superpositions of ^{2}H NMR spectra with different quadrupolar splittings from different positions along the palmitoyl chains. Despite the superposition of different quadrupolar spectra, the 2D pattern does provide a qualitative picture of the motion of the lipid molecules. For example, direct information on the diffusive motions discussed in the previous section is obtained from the extremities of the contour plots. This "plateau" region is due to a closely spaced group of the largest ^{2}H NMR splittings [1] and gives a direct indication of the range of important reorientational angles β in $P^*(\beta;t_m)$.

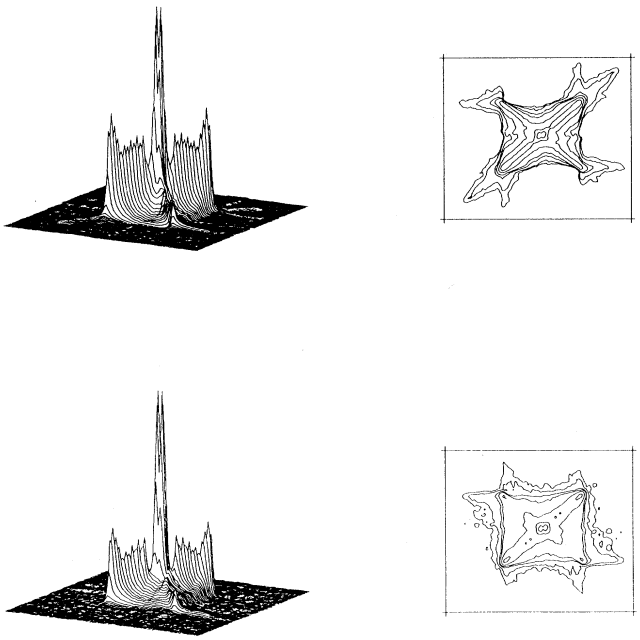

FIG. 4. Stacked plots and their corresponding contour plots for 2D exchange ^{2}H NMR spectra of a multilamellar sample of POPC-d_{31} at 30 °C in the fluid phase for $t_m=1.0$ ms (top) and $t_m=10$ ms (bottom). The plots of both the stacked and contour plots range from -47 to $+47$ kHZ in each dimension. The abscissae correspond to the frequencies $f_1=\omega_1/2\pi$ and the ordinates to $f_2=\omega_2/2\pi$.

In the $t_m=1.0$ ms spectrum, the observation of important "shoulders" on the main diagonal (i.e., the roll off of the distribution of the maximum splittings at $\theta=0°$) tells us that a substantial fraction of molecules has experienced only very small changes in orientation in 1 ms. Roughly speaking, these would correspond to the 30% of the molecules for which $0\leq\beta\leq 6°$ in Sec. IV. The same spectrum also indicates "connections" between "shoulders" on the main diagonal and the "edges" (unsymmetric peaks of intensity corresponding to $\theta=0°$) of the plateau region. This tells us that another substantial group of molecules has experienced reorientations of local surface normals as large as $\beta=90°$. When t_m is increased to $t_m=10$ ms, the exchange is more pronounced since the shoulders on the main diagonals are no longer visible.

These results, based on a qualitative analysis of the 2D exchange ^{2}H NMR spectrum of the 31 palmitoyl deuterons confirms that there are diffusive motions of POPC molecules along curved surfaces in the L_α phase of a similar complexity to those of DPPC as described in the previous section and analyzed using specifically deuterated molecules. Unfortunately, quantitative analysis of the POPC-d_{31} spectra has not been successful. The reasons for this are not completely understood by us at the present time. We suppose that it is due to the difficulty of extracting $P^*(\beta;t_m)$ in the presence of overlapping powder patterns where specific ridges containing valuable information on the reorientational process are obscured by intense ridges parallel to the frequency axis that are not sensitive to the reorientational motions [19], i.e., overlapping of 2D spectra associated with nuclei having different quadrupolar splittings with those from different groups of molecules having different reorientational motions (different indices i in the analysis of Sec. IV). Further work is required to clarify the conditions under which information may be extracted on 2D exchange NMR from complex NMR spectra.

VI. CONCLUDING REMARKS

In this paper, the method of 2D exchange ^{2}H NMR has been applied to the study of lipid bilayer model membranes in the fluid (liquid crystalline) phase. This technique was extensively developed by Spiess and his collaborators [8–11,14,18,19] over a number of years with applications to slow molecular reorientation in polymers and molecular solids. It has also been applied previously [20,21] to the study of both the gel and fluid phases of lipid bilayer membranes of the type studied here.

A special feature of ^{2}H NMR in fluid membranes is that, as a result of the effect of motional averaging over molecular conformations, the spectral frequency is related in an explicit and simple manner to the angle θ between the local membrane surface normal **n** and the externally applied magnetic field. For this reason the 2D spectrum $S(\omega_1,\omega_2;t_m)$ provides a direct measure of the two-time correlation function $P(\theta_1,\theta_2;t_m)$ for local surface normal orientation. For powder samples such as those studied in this paper, such data can be analyzed independently of an explicit model to give the one-

dimensional distribution function $P(\beta;t_m)$ for the rotation of **n** during t_m. This is how we have analyzed our data. Such a characterization of the space and time variation of membrane curvature is of great current interest in the study of geometrical and dynamic aspects of membrane curvature and we believe that the measurements reported here will stimulate further exploration in this area.

As discussed in detail in Sec. IV, our results exhibit the influence of local surface roughness as well as departures from sphericity on distance scales large in relation to the average radius of curvature of the liposomes. This behavior is quite different from that observed for membranes constrained to sphericity by a solid spherical support as reported in the accompanying paper [7].

ACKNOWLEDGMENTS

This research has been supported by the Natural Sciences and Engineering Research Council of Canada and by the Canadian Institute for Advanced Research.

[1] M. Bloom, E. Evans, and O. G. Mouritsen, Q. Rev. Biophys. **24**, 293 (1991).
[2] R. Lipowsky, Nature (London) **349**, 475 (1991).
[3] M. Bloom and J. L. Thewalt, Chem. Phys. Lipids **73**, 27 (1994).
[4] L. Miao, U. Seifert, M. Wortis, and H.-G. Döbereiner, Phys. Rev. E **49**, 5389 (1994).
[5] F. Brochard and J. F. Lennon, J. Phys. (Paris) **36**, 1035 (1975).
[6] M. Bloom and E. Evans, in *Biologically Inspired Physics,* edited by R. Peliti (Plenum, New York, 1991), pp. 137–147.
[7] C. Dolainsky, M. Unger, M. Bloom, and T. Bayerl, following paper, Phys. Rev. E **51**, 4743 (1995).
[8] S. Wefing and H. W. Spiess, J. Chem. Phys. **89**, 1219 (1988).
[9] S. Wefing, S. Kaufmann, and H. W. Spiess, J. Chem. Phys. **89**, 1234 (1988).
[10] S. Kaufmann, S. Wefing, D. Schaefer, and H. W. Spiess, J. Chem. Phys. **93**, 197 (1990).
[11] D. Grabowski and J. Honerkamp, J. Chem. Phys. **96**, 2629 (1992).
[12] J. H. Davis, Biophys. J. **27**, 339 (1979).
[13] E. Sternin, Rev. Sci. Instrum. **56**, 221 (1985).
[14] C. Schmidt, B. Blümlich, and H. W. Spiess, J. Magn. Reson. **79**, 269 (1988).
[15] D. I. Hoult and R. E. Richards, Proc. R. Soc. London **344**, 311 (1975).
[16] J. H. Davis, K. R. Jeffrey, M. Bloom, M. I. Valic, and T. P. Higgs, Chem. Phys. Lett. **79**, 390 (1976).
[17] J. H. Davis, Biochim. Biophys. Acta **737**, 117 (1983).
[18] A. Hagemeyer, L. Brombacher, K. Schmidt-Rohr, and H. W. Spiess, Chem. Phys. Lett. **167**, 583 (1990).
[19] C. Schmidt, S. Wefing, B. Blümlich, and H. W. Spiess, Chem. Phys. Lett. **130**, 84 (1986).
[20] M. Auger and H. C. Jarrell, Chem. Phys. Lett. **165**, 162 (1990).
[21] D. Fenske and H. C. Jarrell, Biophys. J. **59**, 55 (1991).
[22] G. Lindblom, H. Wennerström, and G. Arvidson, Int. J. Quantum. Chem. **12**, Suppl. 2, 153 (1977).
[23] M. Bloom, C. Morrison, E. Sternin, and J. L. Thewalt, in *Pulsed Magnetic Resonance: NMR, ESR and Optics, A Recognition of E. L. Hahn,* edited by D. M. S. Bagguley (Clarendon, Oxford, 1992), pp. 274–316.
[24] F. A. Nezil, C. Morrison, K. P. Whittall, and M. Bloom, J. Magn. Reson. **93**, 279 (1991).
[25] M. Bloom, E. E. Burnell, S. B. W. Roeder, and M. I. Valic, J. Chem. Phys. **66**, 3012 (1977).
[26] M. Bloom and E. Sternin, Biochemistry, **26**, 2101 (1987).